Brazilian Journal
of Chemical
Engineering

ISSN 0104-6632
Printed in Brazil
www.abeq.org.br/bjche

Vol. 36, No. 01, pp. 439 - 452, January - March, 2019
dx.doi.org/10.1590/0104-6632.20190361s20180074

MODEL PREDICTIVE CONTROL FOR PRODUCTION OF ULTRA-LOW SULFUR DIESEL IN A HYDROTREATING PROCESS

José I. S. da Silva[1*] and Argimiro R. Secchi[1]

[1] Universidade Federal do Rio de Janeiro, Programa de Engenharia Química, Rio de Janeiro, RJ, Brasil.
E-mail: josesilva@peq.coppe.ufrj.br, ORCID: 0000-0001-5237-6120; ORCID: 0000-0001-7297-3571

(Submitted: February 21, 2018 ; August 17, 2018 ; Accepted: August 18, 2018)

Abstract - There is a continual desire around the world to reduce the sulphur content of diesel fuel to ultra-low levels (below 10 ppm) due to environmental concerns and the intention of improving air quality and lowering harmful exhaust emissions of diesel engines. In this work, a hydrodesulfurization unit fed with multiple diesel streams was addressed using a phenomenological mathematical model aiming to produce Ultra-Low Sulfur Diesel (ULSD). A three-phase model of a trickle-bed reactor was considered. A model-based predictive control strategy (MPC) was implemented with the objective of controlling the sulfur concentration at the exit of the reactor, manipulating the flow rates of the oils entering the system, the superficial velocity of the gas and the temperature of the load in the presence of disturbances in the concentration of organic sulfur compounds in the fed oils. It was observed that the control strategy reduced the contaminant content to the specification range of diesel S10.
Keywords: Hydrodesulfurization; Ultra-Low Sulfur Diesel; MPC.

INTRODUCTION

The desired performance from process plants is increasingly complicated. Issues such as environmental problems that require care, economic needs, safety requirements, among others, are important factors that influence the quality specifications of industrial products. The integration between industrial processes makes modern processing plants harder to operate. These factors contribute to the argument that the area of process control is of great interest and importance (Carelli and Souza Jr., 2009).

The content of contaminants affects the quality of diesel oil, generating impacts on its commercialization. The amount of these contaminants present in the diesel must comply with the regulations of the fuel sector worldwide (Li et al., 2013). In recent years, environmental issues have become an important subject in discussions around the world, raising the cravings for strong pollution control legislation, especially when it comes to emissions from the use of petroleum products (Ferreira et al., 2013; Ali, 2014). The diesel that meets these recommendations is ULSD (Ultra Low Sulfur Diesel), which contains a maximum of 10 ppm in terms of sulfur in its composition. The production of this fuel requires the intensive use of hydrotreatment (HDT) units, with the need for catalysts of high activity and severe operating conditions (Pacheco et al., 2011; Ferreira et al., 2013).

In order to attend the environmental regulations which limit sulfur content, many countries are investing to produce diesel fuel with ultra-low sulfur levels, focusing on deep desulfurization. This approach also aims to find cost-effective methodology for ultra-low sulfur diesel (ULSD) (Ali, 2014). Advances in ULSD production continue attracting research interest around the world from the scientific and applied points of view. In this way, Stanislaus et al. (2010) discussed

* Corresponding author: José I. S. da Silva - E-mail: josesilva@peq.coppe.ufrj.br

evolution in deep hydrodesulfurization (HDS) processes, emphasizing catalysts and advancement in the hydrotreatment of diesel.

One of the most difficult ways to achieve success in diesel hydrotreating is to operate the plant observing different conditions such as product prices and feed that changes constantly (Adetola and Guay, 2010; Jarullah et al., 2011). The diesel HDT is usually carried out in a Trickle Bed Reactor (TBR), reducing sulfur content and other contaminants (Li et al., 2013). This operation in a TBR is a typical transport-reaction process, characterized by spatial variations and nonlinearities due to the complex reaction mechanisms and diffusion and convection phenomena (Dubljevic et al., 2005). Predictive control strategies can be formulated and implemented and their objectives can be achieved with the use of dynamic models of transport-reaction processes (Dubljevic and Christofides, 2006).

To meet the existing specifications that determine the contaminant content in diesel, the HDT process needs to be controlled, aiming at greater profitability of the operation. Predictive Control (MPC or Model Predictive Control) is considered the most general way to control a process subject to constraints, capable of operating for long periods of time with little intervention (Ogunnaike and Ray, 1994; Seborg et al., 2004; Carelli and Souza Jr., 2009).

Lababidi et al. (2004) studied the application of constrained MPC in a diesel HDT pilot plant from the atmospheric distillation fractionation of petroleum, considering the HDS reaction. In their studies, the authors focused on producing oil with the desired amounts of contaminants. The controller was experimentally assembled to optimize the reaction zone temperatures, resulting in improved process efficiency with respect to desulphurization.

Carelli and Souza Jr (2009) studied Generalized Predictive Controllers (GPC), evaluating the controller performance with monitoring and diagnosis methods based on historical benchmarks and model-based performance measurements. These methods were applied to situations of degraded performance simulated in the predictive control of a diesel hydrotreating reactor.

For this purpose, few references were found in the literature addressing the model predictive control of the HDT process of diesel, as well as for the classical controls for the diesel HDT process. Aiming to contribute to the development of the sector, the objective of this work was to propose a predictive control strategy for the diesel HDT process, aiming to control the sulfur content at the exit of the TBR, in order to obtain Ultra-Low Sulfur Diesel (ULSD) specifications, keeping the sulfur concentration in the product below the maximum value allowed by the legislation.

The reactor mathematical model and the formulated MPC approach are presented first. The results are then discussed and the main conclusions are stated.

PROBLEM FORMULATION

In this work, we considered a multiple feed diesel HDT, addressing the reaction of hydrodesulfurization (HDS), with a irreversible reaction and the organic sulfur content and the hydrogen concentration having a positive effect (Korsten and Hoffman, 1996). A mathematical model of a trickle-bed reactor TBR) was implemented in EMSO (Environment for Modeling, Simulation and Optimization), which is an equation-oriented process simulator available at <http://www.enq.ufrgs.br/alsoc>.

Details of the schematic diagram of the process are shown in Fig. 1, in which three types of vacuum gas oil, VGO, (oil A, oil B and oil C) are available to feed the catalytic reactor (TBR). A Model Predictive Controller (MPC) can also be seen, in which the concentration of organic sulfur compounds at the exit of the TBR can be controlled, manipulating the oil flow-rates in the mixer, the hydrogen flow-rate, and the TBR inlet temperature. We consider that the concentration of organic sulfur compounds is the main difference in the oils A, B and C. The oils are blended in the mixer to adjust the feed composition. The heated oils are saturated with hydrogen and inserted on top of the TBR. The removed organic sulfur leaves the reactor in the gas phase, and the treated oil is obtained in the liquid phase at the bottom of the reactor. The following assumptions were taken into account to model the reactor in order to run the process:

a) Cocurrent operation with hydrogen saturated feed;
b) Three-phase system: gas, liquid and solid phases;
c) Pilot scale operation;
d) Constant operating pressure;
e) Dynamic process model;
f) One-dimensional mathematical model;
g) Two interfaces (gas-liquid and liquid-solid) through which mass transfer occurs;
h) The reactions occur on the surface of the catalyst (in the solid phase);
i) There are no radial gradients of concentration and temperature;
j) The velocities of the liquid and gaseous phases are constant along the reactor.

In order to solve the problem, some parameters and mathematical correlations were taken from the literature in Korsten and Hoffmann (1996), Mederos and Ancheyta (2007), Jimenez et al. (2007), Liu et al. (2008), Alvarez and Ancheyta (2008a), Alvarez and

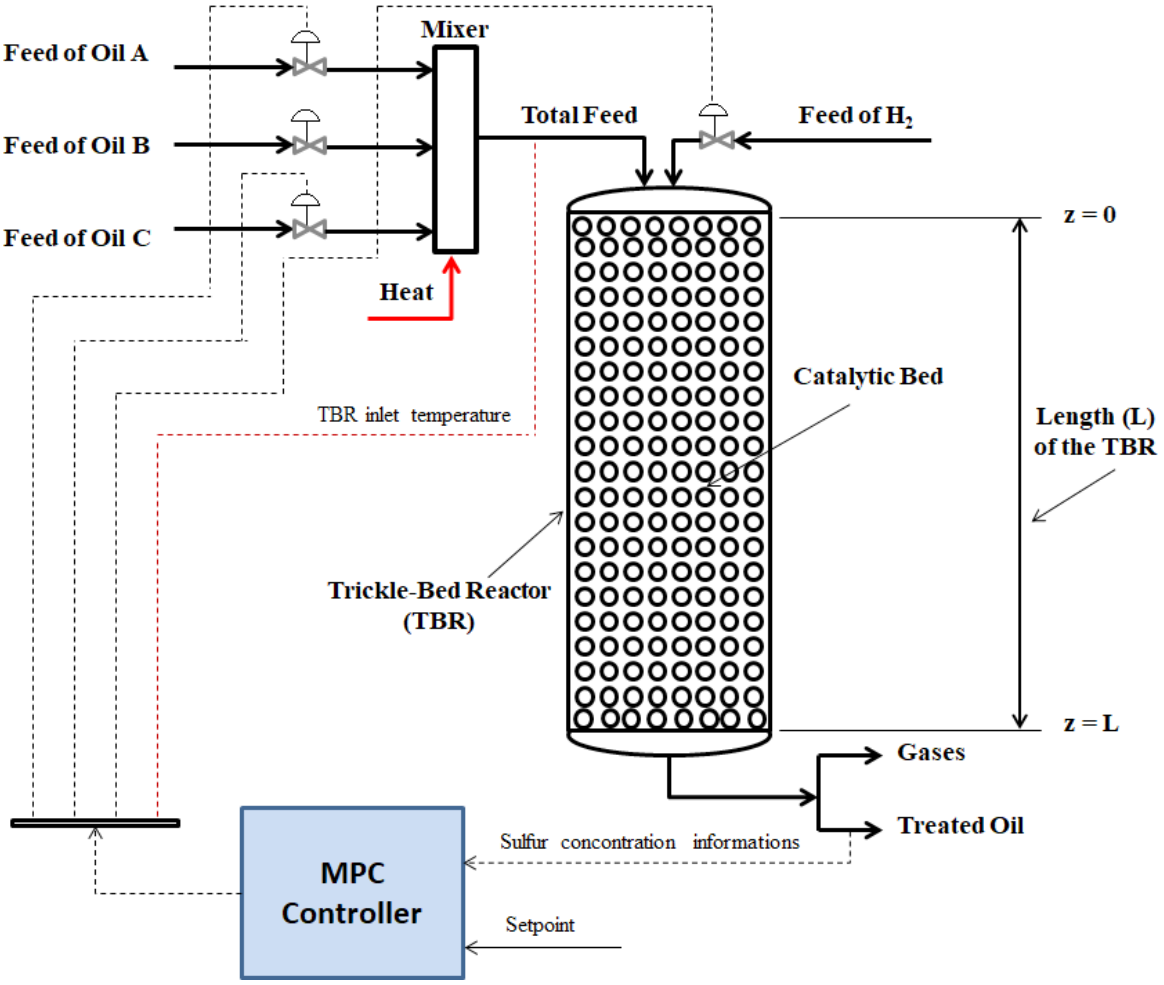

Figure 1. Schematic diagram of the TBR, representing the cocurrent operation of the diesel HDT process.

Ancheyta (2008b), Kallinikos et al. (2010), Alvarez et al. (2011) and Mederos et al. (2012), and are sumarized in the Appendix. The API grade of the oils was considered to be equal to 22 and the molecular weight equal to 441.9 kg/kmol (Mederos and Ancheyta, 2007).

The input data and the operating conditions prior to the MPC and the costs (ANP, 2017) are presented in Table 1. The hydrocarbon concentrations of the oils A, B and C were kept constant and equal to 4.93 (mol cm^{-3}), 3.85 (mol cm^{-3}) and 2.89 (mol cm^{-3}), respectively. The

Table 1. Information about the system studied.

System information	Values
Feed (cm^3/s)	0.03 (oil A) Mass balance (oil B) 0.02 (oil C) 0.1 (TBR inlet)
Organic sulfur concentration (ppm)	400 (oil A) 300 (oil B) 200 (oil C)
Costs (US$/$cm^3$)	1.3×10^{-3} (oil A) 1.4×10^{-3} (oil B) 1.5×10^{-3} (oil C) 2.0×10^{-3} (hydrogen)
Costs of heat in the mixer (US$/kJ)	3.0
T_{MABP} - Average boiling temperature (°C)	476
Surface gas velocity (cm/s)	0.28
Length of the TBR (cm)	35
Equivalent particle diameter (cm)	2.54×10^{-1} (catalyst $CoMo/Al_2O_3$)
Operational pressure (MPa)	5.3
Liquid Hourly Space Velocity, LHSV, (h^{-1})	1

inlet concentration of the reactor is obtained through mass balance.

In the following sections, we present the mathematical modeling of the addressed system.

Mass Balance

In the mixer

Overall and component mass balances in the mixer are given by Equation 1 and Equation 2, respectively, where $F_{total\ feed}$ ($cm^3\ s^{-1}$) is the total feed flowrate of the reactor; $F_{Oil\ A}$ ($cm^3\ s^{-1}$), $F_{Oil\ B}$ ($cm^3\ s^{-1}$) and $F_{Oil\ C}$ ($cm^3\ s^{-1}$) are, respectively, the feed flowrates of oils A, B and C in the mixer; $C_{total\ feed}$ (mol cm^{-3}) is the inlet sulfur concentration of the reactor; $C_{Oil\ A}$ (mol cm^{-3}), $C_{Oil\ B}$ (mol cm^{-3}) and $C_{Oil\ C}$ (mol cm^{-3}) are the sulfur concentrations of the oils in the mixer.

$$F_{total\ feed} = F_{Oil\ A} + F_{Oil\ B} + F_{Oil\ C} \tag{1}$$

$$C_{total\ feed}F_{total\ feed} = C_{Oil\ A}F_{Oil\ A} + C_{Oil\ B}F_{Oil\ B} + C_{Oil\ C}F_{Oil\ C} \tag{2}$$

In the reactor

Based on the works of Mederos and Ancheyta (2007), the following mass balance equations were considered in the TBR, where *t* is the time (s); ε_G is the holdup of gas phase; p_i^G (MPa) is the partial pressure of component i; u_G ($cm\ s^{-1}$) is the gas velocity; z (cm) is the spatial variable; R ($J\ mol^{-1}\ K^{-1}$) is the gas constant; T_G (K) is the temperature of the gas phase; k_i^L ($cm\ s^{-1}$) is the mass transfer coefficient of the component i at the liquid interface; a_L (cm^{-1}) is the specific area at the liquid interface; H_i (MPa cm^3 mol^{-1}) is the constant of Henry's law for component i; C_i^L (mol cm^{-3}) is the concentration of component i in the liquid phase; H_2 is hydrogen gas; H_2S is hydrogen sulfide gas; ε_L is the liquid phase holdup; u_L ($cm\ s^{-1}$) is the velocity of the liquid; D_a^L ($cm^2\ s^{-1}$) is the mass dispersion coefficient in the liquid phase; k_i^S ($cm\ s^{-1}$) is the mass transfer coefficient of component i at the interface of the solid phase; a_S (cm^{-1}) is the specific area at the interface of the solid phase; C_i^S (mol cm^{-3}) is the concentration of component i in the solid phase; S with subscript i represents the sulfur compound and HC represents the hydrocarbons; r_{HDS} (mol $g^{-1}\ s^{-1}$) is the rate of the HDS reaction; the "±" sign means "-" for reagents and "+" for the products; ρ_B (g cm^{-3}) is the bulk density; ξ is the volume fraction of the diluted bed; η_{HDS} is the catalytic efficiency for the HDS reaction; $\in$ is the void fraction in the bed; ε_p is the porosity of the catalyst particle; ρ_B (g cm^{-3}) is the bulk density is the catalytic efficiency for the HDS reaction.

- *Gas phase:*

$$\varepsilon_G \frac{\partial p_i^G}{\partial t} + u_G \frac{\partial p_i^G}{\partial z} + RT_G k_i^L a_L \left(\frac{p_i^G}{\mathcal{H}_i} - C_i^L \right) = 0 \tag{3}$$

i = H_2 and H_2S

- *Liquid phase:*

$$\varepsilon_L \frac{\partial C_i^L}{\partial t} + u_L \frac{\partial C_i^L}{\partial z} - \varepsilon_L D_a^L \frac{\partial^2 C_i^L}{\partial z^2} - k_i^L a_L \left(\frac{Pi}{\mathcal{H}_i} - C_i^L \right) = 0 \tag{4}$$

i = H_2 and H_2S

$$\varepsilon_L \frac{\partial C_i^L}{\partial t} + u_L \frac{\partial C_i^L}{\partial z} - \varepsilon_L D_a^L \frac{\partial^2 C_i^L}{\partial z^2} - k_i^S a_S \left(C_i^L - C_i^S \right) = 0 \tag{5}$$

i = HC and S

- *Solid phase:*

$$\varepsilon_p \left(1 - \in\right) \frac{\partial C_i^S}{\partial t} - k_i^S a_S \left(C_i^L - C_i^S \right) \pm \rho_B \zeta \eta_{HDS} r_{HDS} = 0 \tag{6}$$

i = H_2, H_2S, HC and S

For the liquid and gas phases, the boundary conditions applied to the differential equations are shown below, where the partial pressures of the gaseous components at the inlet of the reactor are:

$$p_i^G = \left(p_i^G \right)_{Z=0}$$

i = H_2 and H_2S

The concentrations of the components in the liquid and solid phases at the inlet of the reactor were based on Danckwerts boundary conditions (Danckwerts, 1995)

$$\left(C_i^L \right)_{Z=0} = \left(C_i^L \right)_0 + \left(\frac{L}{Pe} \right) \left(\frac{\partial C_i^L}{\partial z} \right)_{Z=0}$$

i = H_2, H_2S, S and HC

$$\left(\frac{\partial C_i^L}{\partial z} \right)_{Z=L} = 0$$

i = H_2, H_2S, S and HC

in which the Peclet number (Pe) was calculated by the Hochman-Effort correlation (Mederos and Ancheyta, 2007) for cocurrent pilot operation, through Equation 7:

$$Pe = 0.034 \left(Re_{liq} \right)^{0.5} 10^{0.003\left(Re_{gas} \right)} \tag{7}$$

where Re_{liq} and Re_{gas} are the Reynolds numbers of liquid and gas phases, respectively.

Energy Balance

In the mixer

The energy balance in the mixer is given by Equation 8, where $h_{total\ feed}$ (kJ kmol^{-1}) is the enthalpy of the feed stream to the reactor; Q (kW) is the heat source in the mixer; $h_{Oil\ A}$ (kJ kmol^{-1}), $h_{Oil\ B}$ (kJ kmol^{-1}) and $h_{Oil\ C}$ (kJ kmol^{-1}) are, respectively, the enthalpies of the oils A, B and C in the mixer.

$$F_{total\ feed}h_{total\ feed} + Q = F_{Oil\ A}h_{Oil\ A} + F_{Oil\ B}h_{Oil\ B} + F_{Oil\ C}h_{Oil\ C} \quad (8)$$

In the reactor

Based on the work of Mederos and Ancheyta (2007), the energy balance equations in the TBR are shown below, where ρ_G (g cm^{-3}), ρ_L (g cm^{-3}) and ρ_S (g cm^{-3}) are respectively the gas, liquid and solid phases densities; C_P^G (J g^{-1} K^{-1}), C_P^L (J g^{-1} K^{-1}) and C_P^S (J g^{-1} K^{-1}) are respectively the specific heat capacities of the gas, liquid and solid; h_{GL} (J s^{-1} cm^{-2} K^{-1}) and h_{LS} (J s^{-1} cm^{-2} K^{-1}) are respectively heat transfer coefficients at the gas-liquid and liquid-solid interfaces; T_L (K) and T_S (K) are respectively the liquid and solid phases temperatures; ΔH_R^{HDS} (J mol^{-1}) is the heat of the HDS reaction.

- *Gas phase:*

$$\varepsilon_G\rho_G C_{PG}\frac{\partial T_G}{\partial t} + u_G\rho_G C_{PG}\frac{\partial T_G}{\partial z} + h_{GL}a_L\left(T_G - T_L\right) = 0 \quad (9)$$

- *Liquid phase:*

$$\varepsilon_L\rho_L C_{PL}\frac{\partial T_L}{\partial t} + u_L\rho_L C_{PL}\frac{\partial T_L}{\partial z} - h_{GL}a_L\left(T_G - T_L\right) + h_{LS}a_S\left(T_L - T_S\right) = 0 \quad (10)$$

- *Solid phase:*

$$\left(1-\in\right)\rho_S C_{Ps}\frac{\partial T_S}{\partial t} - h_{LS}a_S\left(T_L - T_S\right) - \rho_B\eta_{HDS}r_{HDS}\left(-\Delta H_{HDS}\right) = 0 \quad (11)$$

For the gas, liquid and solid phases, the boundary conditions applied to the differential equations are shown below, where the temperatures of each phase at the inlet of the reactor are:

At z = 0: $T_L = T_S = To$ and $T_G = 653$ K

Kinetic model

In order to represent the reaction process in this study, we consider the hydrodesulfurization reaction to be irreversible, the organic sulfur content and the hydrogen concentration have a positive effect and, during reaction, hydrogen sulfide is adsorbed at the active catalyst sites. The oil fraction feeding the mixer contains a great amount of organic sulfur compounds (Korsten and Hoffman, 1996).

Usually the overall hydrodesulfurization reaction is represented by the practical and generalized stoichiometric equation. This concept is extensively accepted and accumulates the reaction of all sulfur compounds (Dibenzothiophene-DBT and its alkyl-derivates) in a simple expression (Korsten and Hoffman, 1996; Bhaskar et al., 2004; Rodríguez and Ancheyta, 2004; Mederos and Ancheyta, 2007; Alvarez and Ancheyta, 2008a). The reaction model in question is of the Langmuir-Hinshelwood type, according to Equation 12, in which r_{HDS} (mol g^{-1} s^{-1}) is the rate of HDS reaction; k_{HDS} (cm^3 g^{-1} s^{-1})(cm^3 mol^{-1})$^{0.45}$ is the apparent constant of the HDS reaction; k_{H_2S} (cm^3 mol^{-1}) is the adsorption constant for H_2S.

$$r_{HDS} = \frac{k_{HDS}C_S^S\left(C_{H_2}^S\right)^{0.45}}{\left[1 + k_{H_2S}\left(C_{H_2S}^S\right)\right]^2} \quad (12)$$

Model Discretization and Numerical Integration

In order to solve the problem, the spatial domain of the partial differential equations was discretized by the finite-differences method. The resulting set of differential-algebraic equations was implemented in EMSO software (Soares and Secchi, 2003) and solved by the DASSLC (Secchi, 2012) numerical integrator, with absolute and relative accuracies of 10^{-8} and 10^{-6}, respectively. The number of discretization points required to obtain the adequate solution was 110, uniformly distributed and determined using the mesh convergence criterion of the absolute difference between the values of the process variables obtained at the discretization points of the refinement mesh k+1 and the values obtained at the discretization points by the refinement mesh k, which must be less than 10^{-5}.

Process Control

Predictive control strategies (MPC) of the process were implemented using Matlab®/Simulink, addressed through an EMSO-Matlab interface.

Model Predictive Control (MPC)

Model-based predictive control strategies were used to control the organic sulfur concentration at the exit of the reactor, manipulating the flow rates of the oils A, B and C, as well as the hydrogen gas velocity and the reactor inlet temperature, in the presence of disturbances in the concentrations of these oils in the mixer. The controller was designed so that the response followed the setpoint, reaching the maximum allowed organic sulfur concentration of 10 ppm.

The objective function of the controller follows the formulation presented in Equation 13, in which the MPC outputs are calculated in order to make the controlled variables follow the setpoint optimally. At each sampling instant, the future outputs of the controller are determined in a way that minimizes the

objective function J, where k is the sampling instant, P is the prediction horizon, m is the control horizon, γ_i is the weight on the square error of the controlled variable at time i, $\hat{y}_i$ is the output predicted by the model at time i, y_{set_i} is the value of the setpoint at time i, λ_j is the suppression factor of motion of the controller output at time j, $\Delta U_j = U_j - U_{j-1}$ is the variation of the controller output at time j. Constraints are imposed as follows: $\hat{y}_{min} \leq \hat{y} \leq \hat{y}_{max}$, $U_{min} \leq U \leq U_{max}$, $\Delta U_{min} \leq \Delta U \leq \Delta U_{max}$, in addition to the equality constraints imposed by the linear prediction model.

$$J = \sum_{i=k+1}^{k+p} \gamma_i \left(\hat{y}_i - y_{set_i} \right)^2 + \sum_{j=k}^{k+m-1} \lambda_j \Delta U_j^2 \qquad (13)$$

The weights of the input variables and the output variable, the sampling time, the prediction horizon, and the control horizon are the parameters that will be tuned.

In Fig. 2 the proposed control structure implemented in Simulink can be visualized, in which an s-function was created (which allows one to call the actual plan in EMSO). In the internal block (PLANT_EMSO), the s-function has been configured with five input variables (u_G, F_A, F_C, F_o and T_o), two output variable (CS_{out} and OF), and a sampling time of 5 seconds. Based on sensitivity analysis, the reactor inlet temperature (T_o), gas velocity (u_G) and diesel flow rates (F_A and F_C) in the mixer were chosen to be the manipulated variables in the proposed MPC control system. The organic sulfur concentration (CS_{out}) at the exit of the reactor was chosen as the controlled variable. From the blends of the oils (A, B and C), the inlet liquid flow-rate (F_o) in the reactor was placed as an input variable to account for possible inlet disturbances in the reactor. F_o is the total feed (Equation 1) and it will be fixed (Table 1). The variation of the manipulated variables F_A and F_C will be compensated by F_B. A cost function (OF) was placed in the structure as being an observed output variable, but not controlled in the process. In this way, a 5x2 scheme (5 inputs and 2 outputs) is observed in Fig. 2, however, in this work, the 4x1 structure (4 inputs and 1 output) was considered for the identification and process control steps. With the MPC structure and limits imposed on the manipulated variables, we can analyze the competition among them, since the flow rates of the oils, the hydrogen superficial velocity, and the reactor inlet temperature can be manipulated simultaneously to obtain a best combination of these values to drive the concentration of organic sulfur compounds at the exit of the reactor within the specification. In fact, this 4x1 structure is one of the advantages of using a MPC instead of PID controller, where it is possible to use more than one degree of freedom to drive the process to the desired operating condition. This configuration is even more attractive when the dynamic responses of the system have different velocities for different input variables, which is the case of the HDT process. Besides, it is well-known that the MPC can deal quite well with constraints. An active constraint removes a degree of freedom of the controller; thus, having additional degrees of freedom the MPC does not lose control of the system, which would happen with the PID when the manipulated variable saturates.

Thus, open-loop tests were performed to obtain input and output data from the plant, which served to

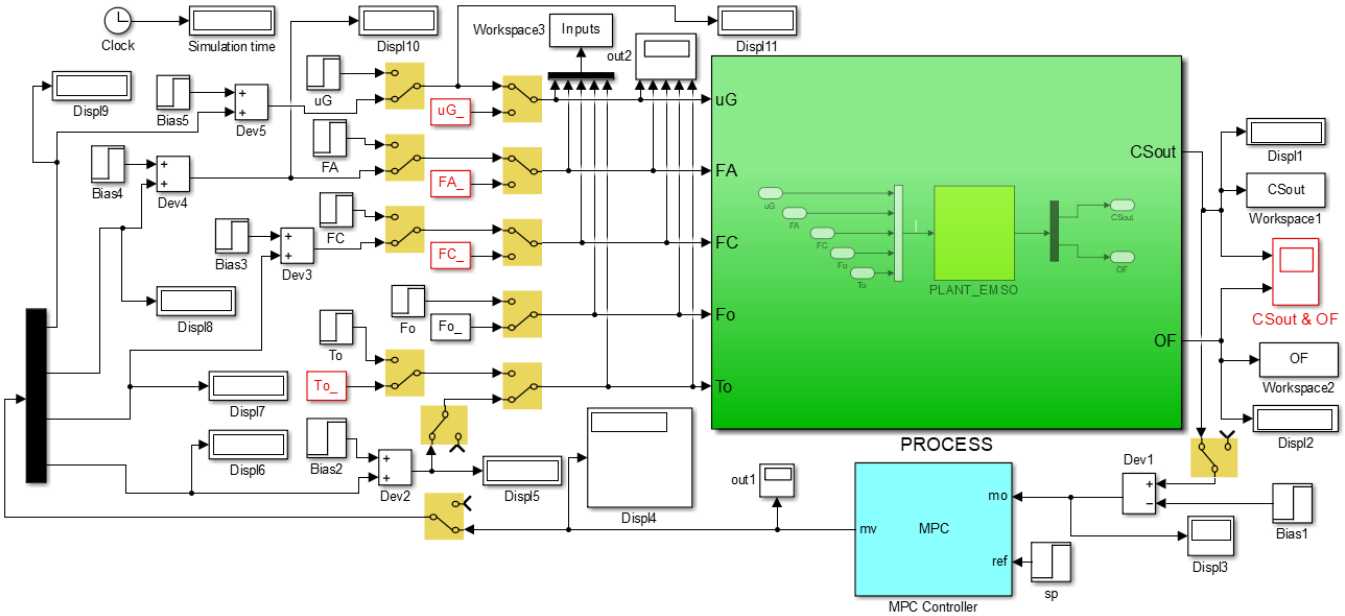

Figure 2. Schematic diagram of the EMSO plant coupled to the Matlab/simulink through the EMSO/Matlab interface.

generate the identified models. Perturbations of 10% in the gas velocity at the reactor inlet, observing the values of the organic sulfur concentration (CS_{out}) at the outlet of the reactor, were taken to the System Identification Toolbox in Matlab, to generate the transfer functions. This procedure was repeated for the other three process inputs.

RESULTS AND DISCUSSION

Model validation

In this work, the operating data from a pilot-scale hydrotreating process were extracted from the work of Mederos and Ancheyta (2007) to validate the mathematical model. The authors considered a single feed diesel HDT process and the assumptions presented in Section 2, with $u_G = 0.028$ cm/s, $u_L = 1.75\times10^{-2}$ cm/s, where u_L is the surface velocity of the liquid phase through the TBR, $T_o = 653$ K and P = 5.3 MPa. The steady-state model was validated in the work of Silva and Secchi (2018). The organic sulfur concentration at the exit of the reactor can be seen in Fig. 3. It is observed that the results obtained in the simulations are similar to the literature, indicating that the reactor model is representative. Mederos and Ancheyta (2007) discussed some HDT operating conditions and showed that cocurrent operation with H_2 saturated oils is the approach which better fits the experimental data. The model parameters provided by these authors were used in this work.

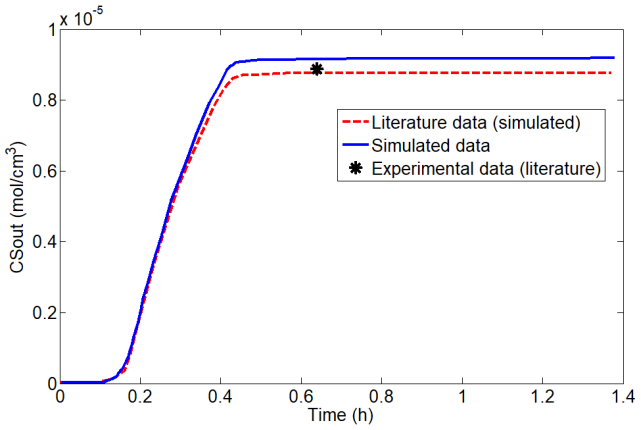

Figure 3. Time evolution of the concentration of organic sulfur compounds (CS_{out}) at the exit of the reactor, simulated data and literature data taken from Mederos and Ancheyta (2007).

Model identification

Open-loop tests were performed to acquire input and output data from the plant to generate the identified model using the System Identification Toolbox in Matlab. The 4x1 structure with the transfer function G (Eq. 14) was built in terms of deviation variables, where g_{11} relates u_G with CS_{out}, g_{21} relates F_A with CS_{out}, g_{31} relates F_C with CS_{out}, and g_{41} relates T_o with CS_{out}. The deviations were established from the following reference values of $u_G = 2.8\times10^{-1}$ cm/s, $F_A = 3.0\times10^{-2}$ cm^3/s, $F_C = 2.0\times10^{-2}$ cm^3/s, $T_o = 653$ K and $CS_{out} = 160$ ppm. The unit of time considered is in seconds, and the units of u_G, F_A and F_C are the same as the ones given in the reference values.

$$G = \begin{bmatrix} g_{11} \\ g_{21} \\ g_{31} \\ g_{41} \end{bmatrix} \tag{14}$$

The identified transfer functions are given in Eqs. 15 to 18 and the quality of the fittings are provided in Table 2.

$$g_{11} = \frac{-2.463\times10^{-5}s^2 - 4.927\times10^{-5}s - 5.565\times10^{-9}}{s^3 + 1.551\times10^{-3}s^2 + 1.93\times10^{-6}s + 9.089\times10^{-11}} \tag{15}$$

$$g_{21} = \frac{9.993\times10^{-5}s^2 - 8.323\times10^{-8}s + 4.603\times10^{-11}}{s^4 + 1.354\times10^{-3}s^3 + 1.188\times10^{-6}s^2 + 5.831\times10^{-10}s + 1.183\times10^{-13}} \tag{16}$$

$$g_{31} = \frac{1.785\times10^{-5}s - 1.079\times10^{-8}}{s^3 + 5.824\times10^{-4}s^2 + 2.163\times10^{-7}s + 3.581\times10^{-11}} \tag{17}$$

$$g_{41} = \frac{-2.662\times10^{-3}s^2 + 6.474\times10^{-6}s - 7.571\times10^{-9}}{s^3 + 2.029\times10^{-3}s^2 + 3.034\times10^{-6}s + 1.48\times10^{-9}} \tag{18}$$

The evaluation of some parameters of the identified models is necessary to attest the quality of the fittings. R^2 greater than 75% means that 50% of the standard deviation of the dependent variable are explained by the model, which is a good result for control purposes. The FPE (Final Prediction Error) value estimates the fit error of the model when predicting new outputs. In order to measure the mean squared errors or deviations, the MSE (Mean Squared normalized Error) value is calculated, which gives the difference between the estimator and what is estimated, corresponding to the quadratic loss value. The MSE is always non-negative and indicates the quality of the estimate. MSE values close to the measurement error indicate a good adjustment of the model to the plant data.

Table 2. Results of the transfer function identifications for the gas velocity (g_{11}), oil A flow rate (g_{21}), oil C flow rate (g_{31}), and reactor inlet temperature (g_{41}).

Criterion	Transfer functions			
	g_{11}	g_{21}	g_{31}	g_{41}
R^2	77.24%	87.12%	82.42%	85.73%
FPE	3.5770×10^{-09}	0.01058	0.005559	1.355
MSE	0.3501	0.01018	0.005099	1.355

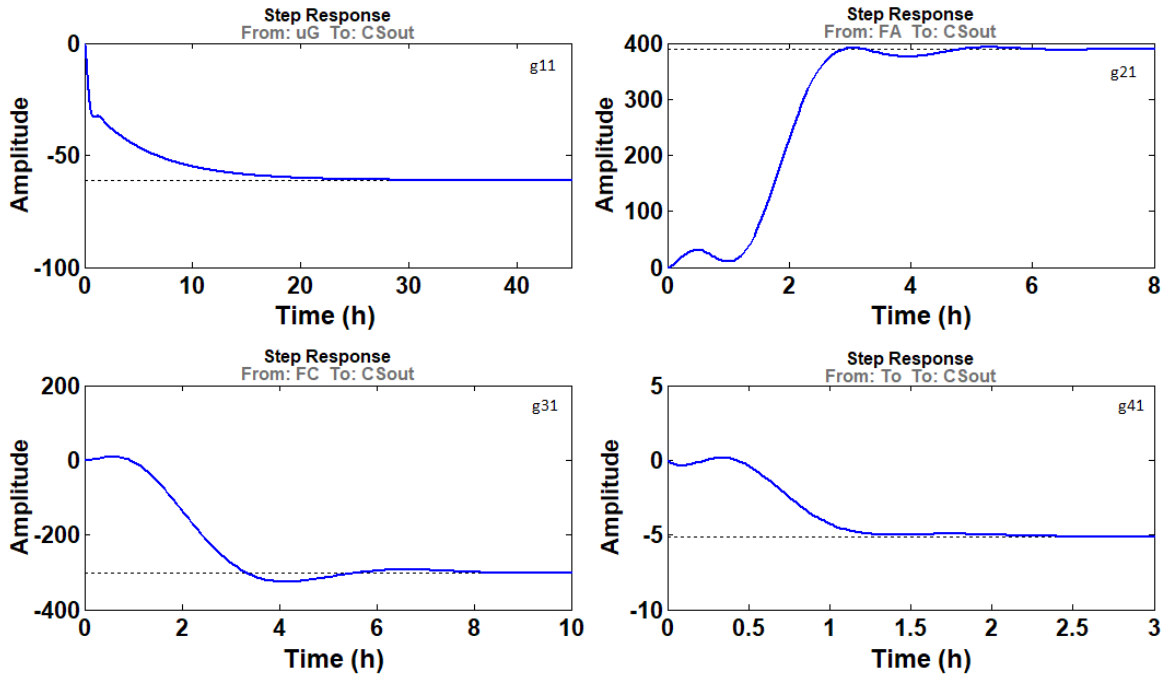

Figure 4. Step response of the identified transfer functions for the process.

Table 2 shows that all R^2 are greater than 75% and the FPE and MSE are relatively small, indicating a good fit to the data and prediction of the identified models.

Step responses of the identified transfer functions are shown in Figure 4, where it can be observed that the stationary gains of the transfer functions are K_{11} = -60, K_{21} = 400, K_{31} = -300 and K_{41} = -5.

Tuning the MPC controller

The MPC was generated from the four identified transfer functions and was implemented in Simulink/Matlab with the process plant in the EMSO simulator.

The tuning of the controller was based on the method of attempts and analysis of the answers, because there is still a shortage of widespread generalized robust methodologies that could be used in the tuning of predictive controllers in general, often applied for specific problems (Garriga and Soroush, 2010; Olesen, 2012).

The tuning of the MPC was carried out in terms of deviation variables in the manipulated (u_G, F_A, F_C and T_o) and in the controlled (CS_{out}) variables from the following reference values of u_G = 2.8×10^{-1} cm/s, F_A = 3.0×10^{-2} cm^3/s, F_C = 2.0×10^{-2} cm^3/s, T_o = 653 K and CS_{out} = 160 ppm. Details of the MPC controller design can be seen in Table 3, which contains the limits on the manipulated variables. The limits on the controlled variables and rate of manipulated variables were left free (MPC toolbox default value).

In the following figures (from Fig. 5 to Fig. 9) we show some results of the MPC tuning, considering the sampling time (ts), prediction horizon (P), control horizon (m), and weights of the manipulated (wm) and controlled (wc) variables.

Table 3. Limits on the manipulated variables.

Variable	Minimum	Maximum
u_G (cm/s)	1.4×10^{-3}	4.8×10^{-1}
F_A (cm^3/s)	1×10^{-2}	4×10^{-2}
F_C (cm^3/s)	1×10^{-2}	4×10^{-2}
T_o (K)	643	706

Fig. 5 shows the actions in the manipulated variables that led the response to follow a setpoint increase of 10 ppm, with the prediction horizon equal to 10, control horizon equal to 2 and sample time equal to 8 minutes. The weights in the manipulated variables were equal to 0 for all variables, and the weight in the output variable was set to 1.

In Fig. 6, the horizons were changed to P = 28 and m = 10. The weights of the manipulated and output variables and the sampling time were kept equal to those in Fig. 5. It was observed that the controller made the response follow a setpoint increase of 10 ppm; however, more oscillations were observed in the controlled and manipulated variables.

In Fig. 7, the parameters P, m, ts and wm were kept equal to those shown in Fig. 6. The weight of the output variable (wc) was changed to 1×10^{-4}. It can be observed that the actions on the manipulated variables easily led the response to follow a setpoint increase of 10 ppm. In this case, it was observed that, upon decreasing wc, the action improves the response, and shows a good performance of the controller.

In Fig. 8, the horizons, sampling time and the weights of the controlled variable were kept equal to those of Fig. 7. The weights of the manipulated variables

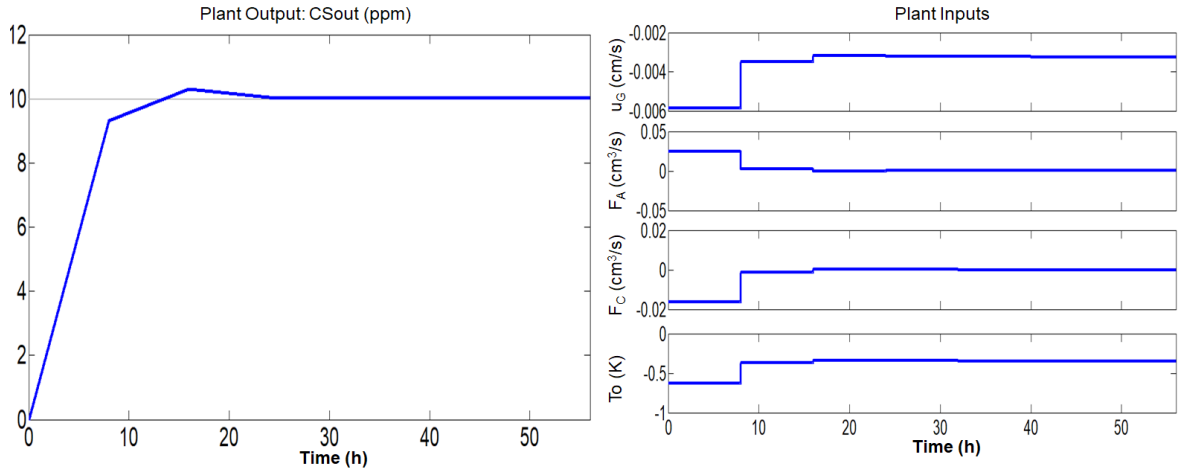

Figure 5. Tuning the MPC controller, in terms of deviation variables in the manipulated (u_G, F_A, F_C and T_o) and in the controlled (CS_{out}) variables. Setpoint increase of 10 ppm, ts = 8 min, P = 10, m = 2, wm = [0, 0, 0, 0], wc = 1. a) Controlled variable, b) Manipulated variables.

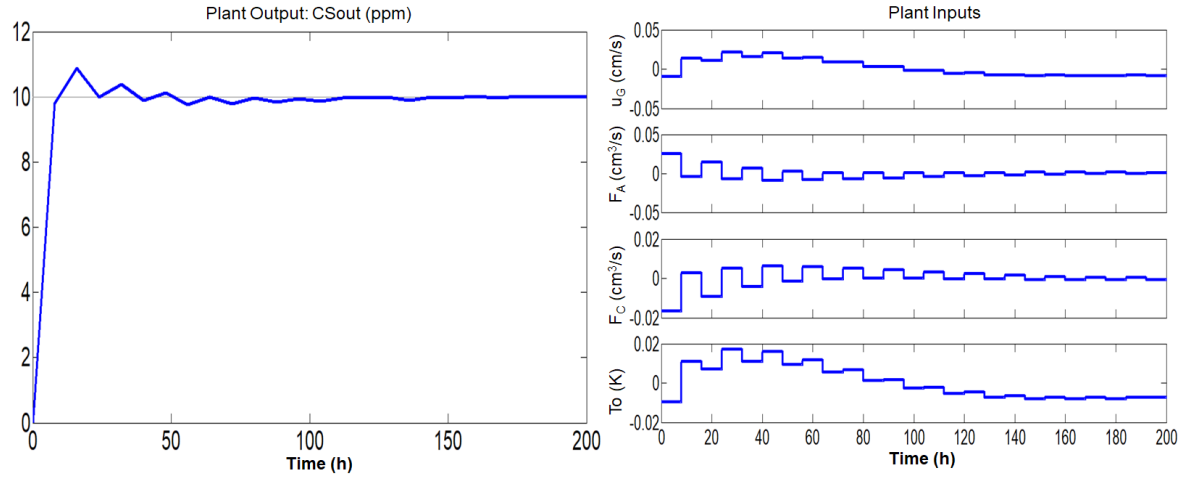

Figure 6. Tuning the MPC controller, in terms of deviation variables in the manipulated (u_G, F_A, F_C and T_o) and in the controlled (CS_{out}) variables. Setpoint increase of 10 ppm, ts = 8 min, P = 28, m = 10, wm = [0, 0, 0, 0], wc = 1. a) Controlled variable, b) Manipulated variables.

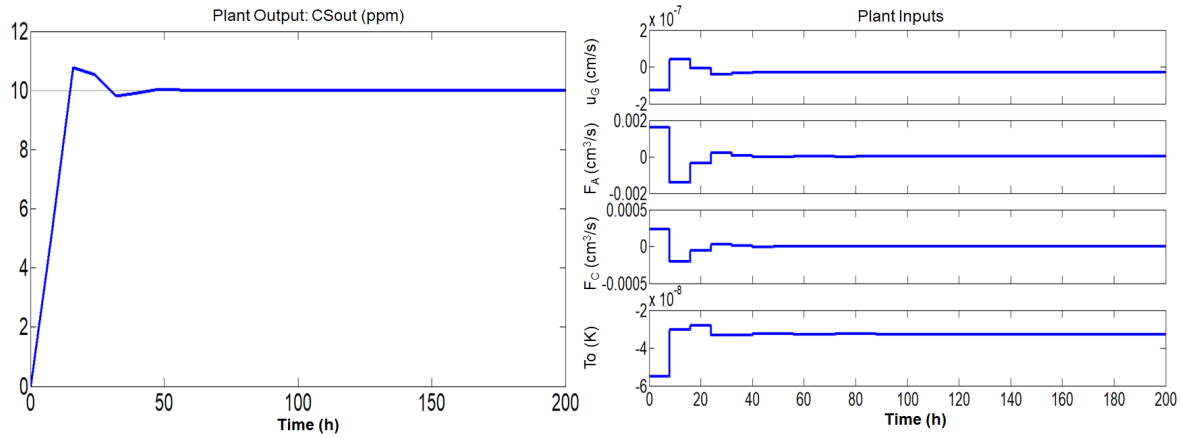

Figure 7. Tuning the MPC controller, in terms of deviation variables in the manipulated (u_G, F_A, F_C and T_o) and in the controlled (CS_{out}) varibles. Setpoint increase of 10 ppm, ts = 8 min, P = 28, m = 10, wm = [0, 0, 0, 0], wc = 1×10^{-4}. a) Controlled variable, b) Manipulated variables.

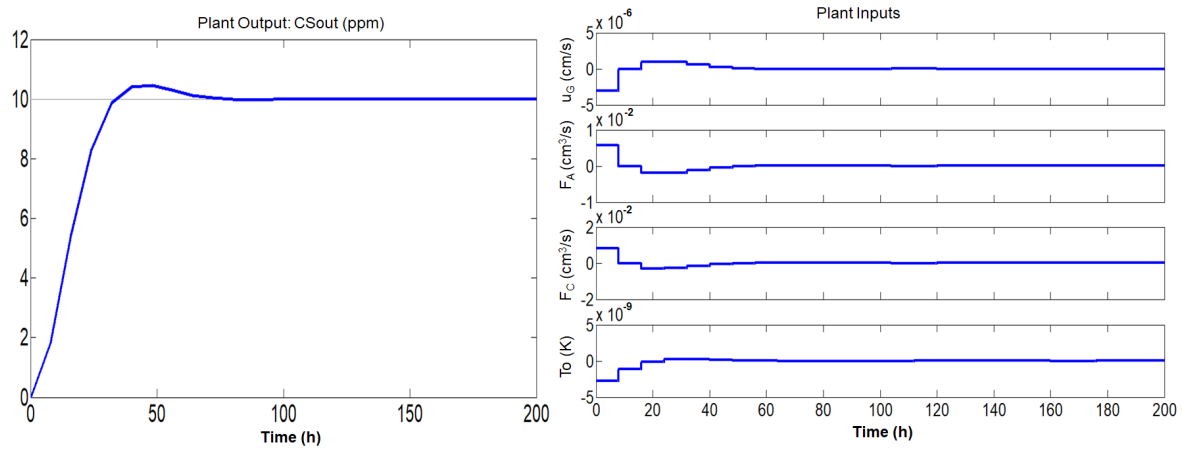

Figure 8. Tuning the MPC controller, in terms of deviation variables in the manipulated (u_G, F_A, F_C and T_o) and in the controlled (CS_{out}) variables. Setpoint increase of 10 ppm, ts = 8 min, P = 28, m = 10, wm = [1, 1, 1, 1], wc = 1×10^{-4}. a) Controlled variable, b) Manipulated variables.

were changed to 1 for all variables. It is noted that the variation of the weights of the manipulated variables improved the performance of the controller and smoothed the response profile, as well as decreasing the weight of the controlled variable as observed in Fig. 7.

Fig. 9 shows the actions in the manipulated variables that led the response to follow a setpoint decrease of 150 ppm (from 160 ppm to 10 ppm). It shows a good performance of the controller. The weights of the manipulated variables were changed to 0 for all variables, and the weight of the controlled variable was set to 0.2.

MPC Applications

Tests were performed to verify the performance of the controller, tuned with the last set of parameters of the previous section, for changes in the operating conditions. The starting condition of the plant was CS_{out} = 160 ppm (in steady state). The performances of the MPC can be observed in the following figures. In Fig. 10, the controller acted satisfactorily, causing the response to follow the setpoint of CS_{out} = 10 ppm after one hour of operation. The manipulated variables u_G, F_A and F_C presented fast responses, reaching their limit values, whereas T_o followed the slow dynamics of the process.

In Fig. 11, the setpoint was changed to 60 ppm at time = 1.4 hour and then was changed again to 10 ppm at time equal to 15h. The variations in the manipulated variables u_G, F_A and F_C occurred rapidly, reaching again their bounds at the first change, whereas in T_o it occurred more slowly due to the relatively slow dynamics regarding to this variable.

For illustrating the effect of the feed sulfur disturbance, Fig. 12 shows disturbances in the concentrations of organic sulfur compounds in the oil streams entering the mixer, seeking to verify effects

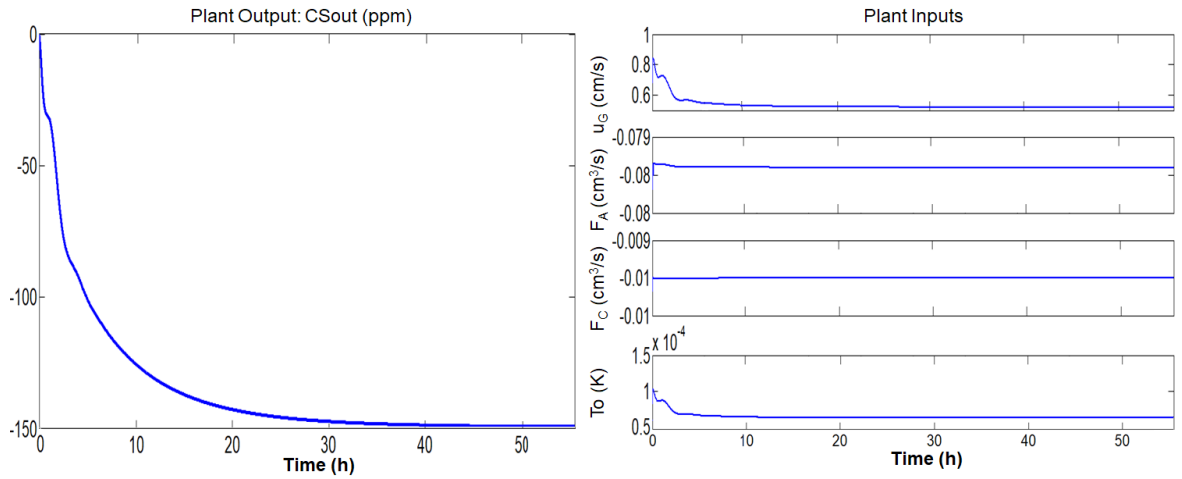

Figure 9. Tuning the MPC controller, in terms of deviation variables in the manipulated (u_G, F_A, F_C and T_o) and in the controlled (CS_{out}) variables. Setpoint decrease of 150 ppm, ts = 8 min, P = 20, m = 10, wm = [0, 0, 0, 0], wc = 0.2. a) Controlled variable, b) Manipulated variables.

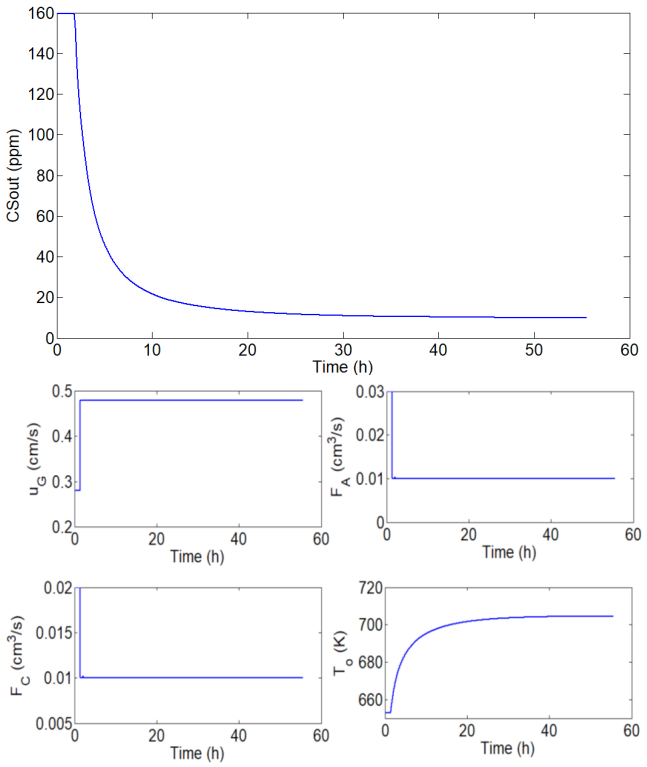

Figure 10. MPC Performance: a) Behavior of the controlled variable (CS_{out}). b), c), d) and e) actuations in the manipulated variables (u_G, F_A, F_C, T_o), causing the response (CS_{out}) to follow the setpoint of CS_{out} = 10 ppm.

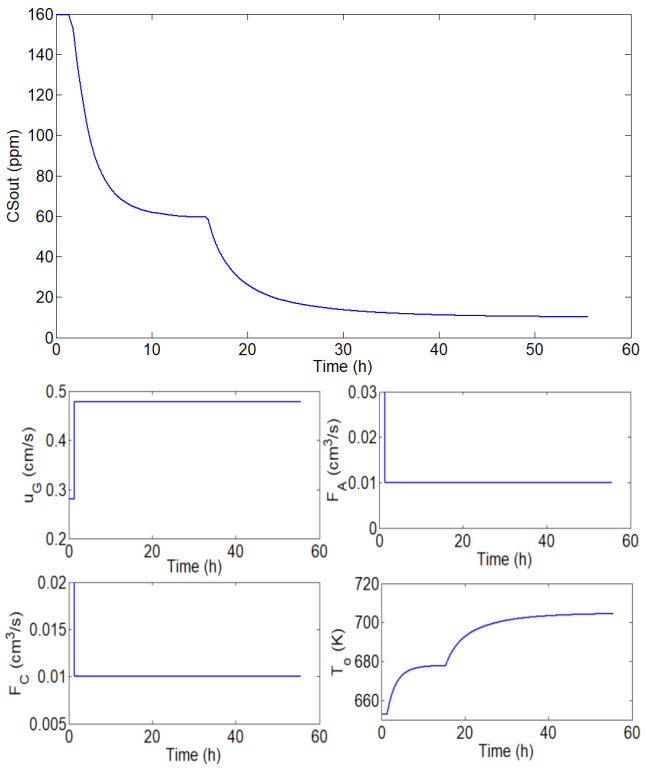

Figure 11. MPC performance: a) Behavior of the controlled variable (CS_{out}). b), c), d) and e) actuations in the manipulated variables (u_G, F_A, F_C and T_o), causing the response (CS_{out}) to follow the setpoint changes (from 160 to 60 ppm at time = 1.4 h, and from 60 to 10 ppm at time = 15h).

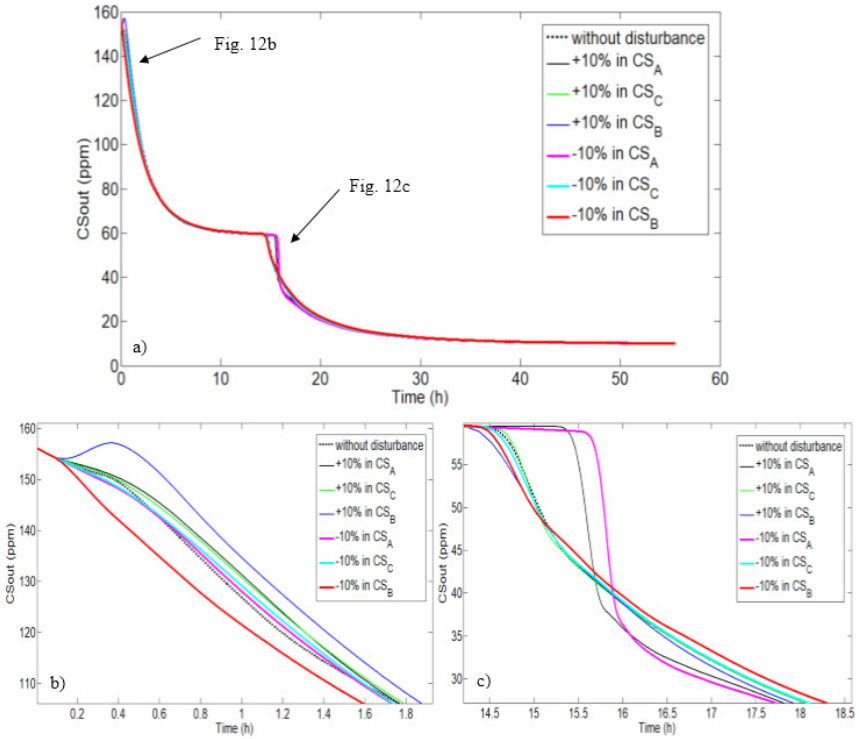

Figure 12. MPC performance: a) Controlled variable (CS_{out}) for setpoint changes (from 160 to 60 ppm at the initial time, and from 60 to 10 ppm at time = 15h) with disturbances (±10) in the inlet oil concentrations at the initial time. b) Details of the response at the beginning of the process; c) Details of the response during the disturbance in the setpoint.

of the change in the concentrations of the oils in the responses, as well as in the MPC performance. Step changes of ±10 in the concentration values of oils A (CS_A), B (CS_B), and C (CS_C). The setpoint was changed to 60 ppm at the initial time and then was changed again to 10 ppm at time equal to 15h. The perturbations in the concentrations of oils A and B were the ones that generated the most differences of the profile without disturbance, which is due to the fact that oil A is the least pure and oil B has the largest flowrate.

The computational time spent in obtaining the model solution was an average of 1 minute. In order to obtain the results of the MPC application, the time was, on average, 20 minutes. The machine used to perform this work was a Dell Core i7 Notebook (Inspiron 14 - 5000 series) with 16GB memory. The EMSO and Matlab versions were, respectively, 0.10.6 and R2014a.

CONCLUSIONS

A hydrodesulfurization unit fed with multiple diesel streams was addressed using a phenomenological mathematical model aiming to produce Ultra-Low Sulfur Diesel (ULSD), in which a three-phase model of a trickle-bed reactor was considered on a pilot scale to implement MPC strategies.

The inlet temperature of the reactor was found to be the most important manipulated variable for the controller's performance to obtain the product within the specifications. In this way, the blend of oils with specific characteristics in the system feed, seeking to meet the product specification is an appreciable alternative to reduce process difficulties. Thus, the blends combined with the possibility of variations in their flow rates and adjustment of the organic sulfur concentration at the TBR inlet can be used to control the diesel hydrotreatment process.

The process responses for setpoint changes and input disturbances in the concentrations of organic sulfur compounds in multiple diesel streams showed that the MPC controller works with good performance.

NOMENCLATURE

$\Delta_{\rho P}$	Pressure dependence of liquid density (g cm^{-3})
$\Delta_{\rho T}$	Temperature correction of liquid density (g cm^{-3})
a_L	Specific surface area at the liquid interface (cm^{-1})
a_S	Specific surface area at the solid interface (cm^{-1})
C_{PL}	Specific heat capacity of the liquid phase (J g^{-1} K^{-1})
$d_{15.6}$	Specific gravity at 15.6 ºC
D_i^L	Molecular diffusivity of compound i in the liquid phase (cm^{-2} s^{-1})
E_a	Activation energy (J mol^{-1})
G_L	Liquid superficial mass velocity (g cm^{-2} s^{-1})
H_i	Henry's law constant for compound i (MPa cm^3 mol^{-1})
j_H	j factor for heat transfer
K_{H_2S}	Adsorption equilibrium constant for H_2S (cm^3 mol^{-1})
k_0 and k_{0,H_2S}	Frequency factors
k_i^L	Mass-transfer coefficient of compound i at the liquid interface (cm s^{-1})
k_i^S	Mass-transfer coefficient of compound i at the solid interface (cm s^{-1})
k_L	Thermal conductivity of the liquid phase (J s^{-1} cm^{-1} K^{-1})
T_L and T_S	Temperatures of the liquid and solid phases (K)
T_{MABP}	Mean average boiling temperature (K)
u_L	Superficial velocity of the liquid phase (cm s^{-1})
v_c^{mix}	Critical specific volume of the liquid mixture (cm^3 mol^{-1})
$v_{i,c}$	Critical specific volume of the gaseous compounds i (cm^3 mol^{-1})
v_i	Molar volume of solute i at its normal boiling temperature (cm^3 mol^{-1})
v_L	Molar volume of liquid solvent at its normal boiling temperature (cm^3 mol^{-1})
v_N	Molar gas volume at standard conditions (NL mol^{-1})
ΔH_{ads}	Adsorption enthalpy of H_2S (J mol^{-1})
ΔH_{HDS}	Heat of hydrodesulfurization reaction (J mol^{-1})
λ_{H_2}	Solubility coefficient of the hydrogen (NL kg^{-1} MPa^{-1})
λ_{H_2S}	Solubility coefficient of the hydrogen sulfide (NL kg^{-1} MPa^{-1})
μ_L	Absolute viscosity of the liquid (mPa s)
ρ_0	Liquid density at standard conditions (g cm^{-3})
ρ_{20}	Liquid density at 20 °C (g cm^{-3})
ρ_L	Liquid density at process conditions (g cm^{-3})
$\in$	Bed void fraction
dp	Equivalent particle diameter (cm)

h_{LS}	Heat-transfer coefficient for the liquid film surrounding the catalyst particle (J s^{-1} cm^{-2} K^{-1})
P	Reactor total pressure (MPa)
R	Universal gas constant (J mol^{-1} K^{-1})

REFERENCES

Adetola, V., and Guay, M., Integration of real-time optimization and model predictive control. Journal of Process Control, 20, 125-133 (2010). http://doi.org/10.1016/j.jprocont.2009.09.001

Ali, S. A. Development of improved catalysts for deep HDS of diesel fuels. Appl Petrochem Res 4: 409-415, 2014. https://doi.org/10.1007/s13203-014-0082-x

Alvarez, A.; and Ancheyta, J., Modeling residue hydroprocessing in a multi-fixed-bed reactor system. Applied Catalysis A: General, 351, 148-158 (2008b). http://doi.org/10.1016/j.apcata.2008.09.010

Alvarez, A.; and Ancheyta, J. Simulation and analysis of different quenching alternatives for an industrial vacuum gasoil hydrotreater. Chemical Engineering Science, 63, 662-673 (2008a). https://doi.org/10.1016/j.ces.2007.10.007

Alvarez, A.; Ancheyta, J.; Centeno, G.; and Marroquín, G. A modeling study of the effect of reactor configuration on the cycle length of heavy oil fixed-bed hydroprocessing. Fuel, 90, 3551-3560 (2011). https://doi.org/10.1016/j.fuel.2011.03.043

ANP - Brazilian National Agency of Petroleum, Natural Gas and Biofuels (Portuguese: Agência Nacional do Petróleo, Gás Natural e Biocombustíveis - ANP). Price Survey System (Sistema de Levantamento de Preços), 2017. In < http://www.anp.gov.br/preco/ >

Bhaskar, M.; Valavarasu, G.; Sairam, B.; Balaraman, K. S.; and Balu, K., Three-Phase Reactor Model to Simulate the Performance of Pilot-Plant and Industrial Trickle-Bed Reactors Sustaining Hydrotreating Reactions. Industrial & Engineering Chemistry Research, 43, 6654-6669 (2004). https://doi.org/10.1021/ie049642b

Carelli, A. C.; and Souza Jr., M. B., Stochastic and Deterministic Performance Assessment of PID and MPC Controllers: Application to a Hydrotreater Reactor. 10th International Symposium on Process Systems Engineering. Computer-Aided Chemical Engineering, 27, 1635-1640 (2009). https://doi.org/10.1016/S1570-7946(09)70663-7

Danckwerts, P. V., Continuous flow systems. Distribution of residence times. Chemical Engineering Science, 50, 3857-3866 (1995). https://doi.org/10.1016/0009-2509(96)81811-2

Dubljevic, S.; and Christofides, P. D., Predictive control of parabolic PDEs with boundary control actuation. Chemical Engineering Science, 61, 6239-6248 (2006). https://doi.org/10.1016/j.ces.2006.05.041

Dubljevic, S.; Mhaskar, P.; El-Farra, N. H.; and Christofides, P. D., Predictive control of transport-reaction processes. Computers and Chemical Engineering, 29, 2335-2345 (2005). https://doi.org/10.1016/j.compchemeng.2005.05.008

Ferreira, A. S.; Nicoletti, M. C.; Bertini, J. R. and Giordano, R. C., Methodology for inferring kinetic parameters of diesel oil HDS reactions based on scarce experimental data. Computers and Chemical Engineering, 48, 58-73 (2013). http://doi.org/10.1021/acs.energyfuels.5b00467

Garriga, J. L.; and Soroush, M., Model Predictive Control Tuning Methods: A Review. Ind. Eng. Chem. Res., 49, 3505-3515 (2010). https://doi.org/10.1021/ie900323c

Jarullah, A. T., Mujtaba, I. M., and Wood, A. S.,, Kinetic model development and simulation of simultaneous hydrodenitrogenation and hydrodemetallization of crude oil in trickle bed reactor. Fuel, 90, 2165-2181 (2011). http://doi.org/10.1016/j.fuel.2011.01.025

Jimenez, F.; Ojeda, K.; Sanchez, E.; Kafarov, V.; and Maciel Filho, R., Modeling of trickle bed reactor for hydrotreating of vacuum gas oils: effect of kinetic type on reactor modeling. Computer Aided Chem. Eng., 24, 515-520 (2007). https://doi.org/10.1016/S1570-7946(07)80109-X

Kallinikos, L. E.; Jess, A.; and Papayannakos, N. G., Kinetic study and H2S effect on refractory DBTs desulfurization in a heavy gasoil. Journal of Catalysis, 269, 169-178 (2010). https://doi.org/10.1016/j.jcat.2009.11.005

Korsten, H.; and Hoffmann, U., Three-Phase reactor model for hydrotreating in pilot tricke-bed reactors. AIChE J., 42, 1350-1360 (1996). https://doi.org/10.1002/aic.690420515

Lababidi, H. M. S.; Alatiqi, I. M.; and Ali, Y. I., Constrained model predictive control for a pilot hydrotreating plant. Chemical Engineering Research and Design, 82, 1293-1304 (2004). https://doi.org/10.1205/cerd.82.10.1293.46740

Li, D.; Li, Z.; Li, W.; Liu, Q.; Feng, Z.; and Fan, Z., Hydrotreating of low temperature coal tar to produce clean liquid fuels. Journal of Analytical and Applied Pyrolysis, 100, 245-252 (2013). https://doi.org/10.1016/j.jaap.2013.01.007

Liu, Z.; Zheng, Y.; Wang, W.; Zhang, Q.; and Jia, L., Simulation of hydrotreating of light cycle oil with a system dynamics model. Applied Catalysis A: General, 339, 209-220 (2008). http://doi.org/10.1016/j.apcata.2008.01.018

Mederos, F. S.; and Ancheyta, J., Mathematical modeling and simulation of hydrotreating reactors: Cocurrent versus countercurrent operations. Appl. Cat. A: General, 332, 8-21 (2007). https://doi.org/10.1016/j.apcata.2007.07.028

Mederos, F. S.; Ancheyta, J.; and Elizalde, I., Dynamic modeling and simulation of hydrotreating of gas oil obtained from heavy crude oil. Appl. Cat. A: General, 425-426, 13-27 (2012). https://doi.org/10.1016/j.apcata.2012.02.034

Ogunnaike, B. A.; and Ray, W. H., Process Dynamics, Modeling, and Control. Oxford University Press, NY, 1994.

Olesen, D. H., Tuning Methods for Model Predictive Controllers. Technical University of Denmark (M.Sc. thesis, IMM-M.Sc.-2012-69), Kongens Lyngby, Denmark, 2012.

Pacheco, M. E.; Salim, V. M. M.; and Pinto, J. C., Accelerated deactivation of hydrotreating catalysts by coke deposition, Industrial and Engineering Chemistry Research 50, 5975-5981 (2011). https://doi.org/10.1021/ie1023595

Rodríguez, M. A.; and Ancheyta, J., Modeling of Hydrodesulfurization (HDS), Hydrodenitrogenation (HDN), and the Hydrogenation of Aromatics (HDA) in a Vacuum Gas Oil Hydrotreater. Energy Fuels, 18, 789-794 (2004). https://doi.org/10.1021/ef030172s

Seborg, D. E.; Edgar, T. F.; and Mellichamp, D., A. Process dynamic and control. United States: Wiley, 2nd Edition, 2004. 713 p.

Secchi, A. R., DASSLC: user's manual - v3.9 (Differential-Algebraic System Solver in C), 2012. Available at: http://www.enq.ufrgs.br/englib/numeric

Silva, J. I. S.; and Secchi, A. R., An approach to optimize costs during ultra-low hydrodesulfurization of a blend consisting of different oil streams. Brazilian Journal of Chemical Engineering. 35, 1289-1300. (2018). https://doi.org/10.1590/0104-6632.20180354s20170370

Soares, R. P.; and Secchi, A. R., EMSO: A new environment for modelling, simulation and optimization. Computer Aided Chemical Engineering, 14, 947-952 (2003). http://doi.org/10.1016/S1570-7946(03)80239-0

Stanislaus, A.; Marafi, A.; and Rana, M. S., Recent advances in the science and technology of ultra low sulfur diesel (ULSD) production. Catalysis Today, 153, 1-68 (2010). http://doi.org/10.1016/j.cattod.2010.05.011

APPENDIX

Model parameters and mathematical correlations were taken from Korsten and Hoffmann (1996), Mederos and Ancheyta (2007), Jiménez et al. (2007), Liu et al. (2008), Alvarez and Ancheyta (2008a), Alvarez and Ancheyta (2008b), Kallinikos et al. (2010), Alvarez et al. (2011) and Mederos et al. (2012), and are summarized in Table A1.

Table A1. Parameters and correlations used in the mathematical model.

Gas-liquid mass-transfer coefficient	$\frac{K_i^L a_L}{D_i^L} = 7\left(\frac{G_L}{\mu_L}\right)^{0.4}\left(\frac{\mu_L}{D_i^L \rho_L}\right)^{0.5}$
Liquid-solid mass-transfer coefficient	$\frac{K_i^S}{D_i^L a_s} = 1.8\left(\frac{G_L}{a_s \mu_L}\right)^{0.5}\left(\frac{\mu_L}{D_i^L \rho_L}\right)^{1/3}$
Liquid-solid heat-transfer coefficient	$h_{LS} = j_H\, c_{pL}\, u_L\, \rho_L \left(\frac{c_{pL}\,\mu_L}{k_L}\right)^{-2/3}$
Oil density	$\Delta\rho_T = (T_L - 520)[0.0133 + 152.4(\Delta\rho_P + \rho_0)^{-2.45}] - (T_L - 520)^2[8.1\times10^{-6} - 0.0622\times 10^{-0.764(\Delta\rho_P+\rho_0)}]$ $\Delta\rho_P = \left(\frac{P}{1000}\right)[0.167 + (16.181\times10^{-0.0425\times\rho_0})] - \left(\frac{P}{1000}\right)^2 \times 0.01[0.299 + (263\times10^{-0.0603\rho_0})]$ $\rho(T_L, P) = \rho_0 + \Delta\rho_P - \Delta\rho_T$
Henry coefficient	$\mathcal{H}_i = \frac{v_N}{\lambda_i \rho_L}$
Specific surface area	$a_s = \frac{6}{dp}(1-\epsilon)$; See Table 1
Diffusivity	$D_i^L = 8.93\times10^{-8}\left(\frac{v_L^{0.267}}{v_i^{0.433}}\right)\left(\frac{T_L}{\mu_L}\right)$
Dynamic viscosity of the liquid	$\mu_L = 3.141\times10^{10}(T_L - 460)^{-3.444}[\log_{10}(API)]^y$ $y = 10.313[\log_{10}(T_L - 460)] - 36.447$
Molar volume	$v_i = 0.285\times v_{i,c}^{1.048}$ $v_c^{mix} = 7.5214\times10^{-3}(T_{MABP}^{0.2896})(d_{15.6}^{-0.7666})$; See Table 1
Solubility of H_2S	$\lambda_{H_2S} = \exp(3.367 - 0.00847\, T_L)$
Solubility of H_2	$\lambda_{H_2} = -0.559729 - 0.42947\times10^{-3}\, T_L + 3.07539\times10^{-3}\left(\frac{T_L}{\rho_{20}}\right) + 1.94593\times10^{-6}T_L^2 + \frac{0.835783}{\rho_{20}^2}$
Kinetic model of HDS reaction	See Equation 12, with E_a= 131993 J/mol; k_0= 4.266×10^9 cm^3/(g s)×(cm^3/mol)$^{0.45}$ and ΔH_{HDS}= -251000 $K_{H_2S} = k_{0,H_2S}\exp\left(\frac{\Delta H_{ads}}{RT_S}\right)$; k_{0,H_2S} = 41770 cm^3/mol; ΔH_{ads}=2761 J/mol